RSC 2025/59
Robert Schuman Centre for Advanced Studies
Global Governance Programme

WORKING PAPER

Deforestation and Infectious Animal Diseases

Cosimo Beverelli, Rohit Ticku

European University Institute
Robert Schuman Centre for Advanced Studies
Global Governance Programme

Deforestation and Infectious Animal Diseases

Cosimo Beverelli, Rohit Ticku

RSC Working Paper 2025/59

ISSN 1028-3625

Published in December 2025 by the European University Institute.
Badia Fiesolana, via dei Roccettini 9
I – 50014 San Domenico di Fiesole (FI)

Italy

With the support of the Erasmus+ Programme of the European Union

The European Commission supports the EUI through the European Union budget. This publication reflects the views only of the author(s), and the Commission cannot be held responsible for any use which may be made of the information contained therein.

Robert Schuman Centre for Advanced Studies

The Robert Schuman Centre for Advanced Studies, created in 1992 and currently directed by Professor Erik Jones, aims to develop inter-disciplinary and comparative research on the major issues facing the process of European integration, European societies and Europe's place in 21st century global politics.

The Centre is home to a large post-doctoral programme and hosts major research programmes, projects and data sets, in addition to a range of working groups and ad hoc initiatives. The research agenda is organised around a set of core themes and is continuously evolving, reflecting the changing agenda of European integration, the expanding membership of the European Union, developments in Europe's neighbourhood and the wider world.

For more information: http://eui.eu/rscas
The EUI and the RSC are not responsible for the opinion expressed by the author(s).

The Global Governance Programme

The Global Governance Programme is one of the flagship programmes of the Robert Schuman Centre. It is a community of outstanding professors and scholars, that produces high quality research and engages with the world of practice through policy dialogue. Established and early-career scholars work on issues of global governance within and beyond academia, focusing on four broad and interdisciplinary areas: Global Economics, Europe in the World, Cultural Pluralism and Global Citizenship. The Programme also aims to contribute to the fostering of present and future generations of policy and deci-sion makers through its executive training programme: the Academy of Global Governance, where theory and 'real world' experience meet and where leading academics, top-level officials, heads of international organisations and senior execu-tives discuss on topical issues relating to global governance.

For more information: http://globalgovernanceprogramme.eui.eu

Abstract

This paper examines how deforestation in the tropics contributes to the spread of infectious animal diseases. Using geo-referenced data on disease outbreaks and forest loss across 60 countries from 2004 to 2018, we show that a 1% increase in deforestation in neighbouring areas leads to a 1.6% rise in animal infections. We perform several tests to rule our omitted variable bias or measurement error. We find that two mechanisms underpin this effect: (i) habitat destruction increases wildlife-livestock interaction, and (ii) deforestation-linked infrastructure enhances market access, facilitating the transmission of pathogens through animal trade. We also investigate potential zoonotic spillovers. While deforestation on average does not translate into zoonotic transmissions, large shocks may contribute to increases in human infections. Our findings quantify a negative externality of land-use change and underscore how global agricultural demand and infrastructure development can create health risks for animals and humans, highlighting a novel trade-o between economic development and biosecurity.

Keywords

Deforestation; disease; live animals; wildlife; trade

JEL Classification

F18; I18; O13; Q23 W

Acknowledgments

Without implicating them, we thank Tindara Addabbo, Nicolas Berman, Francesco Dragho, Matteo Fiorini, Bernard Hoekman, Gianluca Ore ce, Daniel Prosi, Fabrizia Mealli, Marcello Morciano, Marcelo Olarreaga, Alessandro Tarozzi, Lore Vandewalle and participants at ETSG Milan workshop and EUI MEWG workshop for useful comments and suggestions. We also thank Nicolas Berman, Mathieu Couttenier, Antoine Leblois and Raphael Soubeyran for sharing the deforestation data. Cosimo Beverelli acknowledges funding from the FAR 2024 per Piani di Sviluppo Dipartimentali, Protocol no. 200586.

1 Introduction

How do global market forces and infrastructure development shape health risks in the agricultural economy? While the benefits of agricultural expansion and improved market connectivity are well documented, their unintended consequences, particularly for animal health, are less understood. In this paper, we identify a novel externality of land-use change: deforestation, that is often driven by global demand for agricultural commodities, significantly increases the spread of infectious diseases among animals, and in some instances spreads to humans.

We focus on tropical regions, where economic incentives to expand cropland are strong, and forest ecosystems are especially vulnerable. Deforestation in these areas is not only an environmental issue; it also reshapes disease dynamics by altering contact patterns between wildlife and livestock and by facilitating the movement of live animals through improved transportation links. These indirect spillovers, mediated through ecological and trade channels, can impose large and persistent costs on agricultural systems dependent on healthy animal populations (Dobson et al., 2020; Ticku and Beverelli, 2023).

We combine geo-referenced data on 31 animal diseases worldwide (Beverelli and Ticku, 2025) with tropical deforestation data (Berman et al., 2023), all mapped onto a uniform grid of $0.5^\circ \times 0.5^\circ$ latitude–longitude cells (roughly 55 km × 55 km at the Equator) covering the period from 2004 to 2018. The resulting dataset captures deforestation events and animal disease outbreaks across roughly 12,000 grid cells over 15 years and includes about 22,000 recorded outbreaks.

Our baseline specification estimates the effect of total deforestation in neighbouring grid cells on the number of animals that are infected through disease outbreaks annually in each cell. Given that the outcome variable is a count and includes a large number of zeros, we use a Poisson Pseudo Maximum Likelihood (PPML) estimator, which is well-suited for panel data and provides consistent estimates under such conditions (Santos Silva and Tenreyro, 2011).

In our baseline model, which is estimated with cell and year fixed effects, a 1% increase in neighbourhood deforestation leads to a 1.6% rise in infected animals (95% confidence interval of 0.9–2.2%). In levels, this corresponds to roughly 161 additional infections per 1,000 hectares of neighbourhood deforestation. The magnitude is consistent with neighbourhood deforestation contributing to the spread of infectious animal diseases, and in countries like Mexico and Taiwan, the implied counts reach tens of thousands animal infections per 1,000 hectares.

Our baseline specification allows us to control for the direct effect of deforestation in a cell, along with other cell-level characteristics that might be correlated with the spread of infectious animal diseases, such as livestock population, the local micro-climate, socio-political indicators, and economic activity. The adverse spillover effect of neighbourhood deforestation remains sizable, while we do not find any evidence that deforestation within a cell is consequential.

We address two concerns that impede a causal interpretation of our findings. We first address concern that omitted variables like evolving agricultural patterns or technological changes might drive both neighbourhood deforestation and infectious diseases. We show that the results are robust to controlling for country-year fixed effects that account for structural changes or technological adoptions across countries. We go a step further and show that the results are robust to inclusion of province-year fixed effects that account for local specificities in these dynamics. Next, we address the concern that countries might vary in their disease surveillance capacity that might be correlated with incentives for deforestation. We show that the results are robust to controlling for the number of animal disease screening and surveillance measures that countries implement over time, thus accounting for reporting differences. Additionally, the baseline PPML results pass through several robustness checks, which includes alternative definition of neighbourhood deforestation exposure, and allowing for distance-based spatially correlated inference. The battery of tests show that neighbourhood deforestation has a robust positive effect on the spread of infectious animal diseases.

We turn to the mechanisms and investigate whether neighbourhood deforestation results in a surge in animal infections through (i) habitat loss increasing wildlife–livestock interactions, and (ii) improved market access through road construction facilitating the movement of live animals. To test the first channel, we restrict the sample to the eight diseases that infect both wild and domestic animals. In this subsample, neighbourhood deforestation remains strongly associated with animal infections, consistent with greater wildlife–livestock contact. A complementary test shows that deforestation raises infections among domesticated animals only when neighbouring cells also report wildlife cases, suggesting that habitat loss drives disease-carrying wildlife into inhabited areas. To test the market-access channel, we interact neighbourhood deforestation with a time-invariant measure of road density. The results indicate that infections rise particularly in areas with greater road connectivity, consistent with disease transmission through animal trade. Although both channels matter, the wildlife–livestock pathway is quantitatively more important than the trade-related one.

Our main analysis quantifies the average contemporanous effect of neighbourhood deforestation

on the spread infectious animal diseases. However, large-scale neighbourhood deforestation might propagate infectious animal diseases whose impact can be long-lasting. We assess these dynamics through an event study, estimating the effect of large neighbourhood deforestation shocks. We identify no pre-trends in the number of animal infections prior to a neighbourhood deforestation shock, and a persistent effect in the years since. The dynamic pattern reinforces the baseline elasticity by revealing that large deforestation shocks in the neighbourhood not only result in higher infections contemporaneously but also propagate medium-run increases in infectious animal diseases.

Though data is limited, we assess whether neighbourhood deforestation can directly impact human health through zoonotic transmissions. In our dataset, zoonotic transmissions are rare events, with approximately one in ten animal disease outbreaks resulting in a human infection. The baseline PPML estimation fails to detect any effect of neighbourhood deforestation on human infections, however event study results suggest that large deforestation shocks may result in zoonotic transmissions. While this evidence highlights the potential for deforestation to contribute to spillovers into humans, we view it as exploratory. More extensive epidemiological data would be needed to establish stronger causal inference.

In the final part of our analysis, we assess if national-level coordination can attenuate the spatial infection externalities that local agents or subnational institutions might not fully internalize. Specifically, we test whether being part of the REDD+ plus group, which requires countries to develop national-level coordination strategies against deforestation, mitigates infection spillovers. Our results suggest that the elasticity of infections with respect to neighbouring deforestation is three times larger in non-REDD+ countries, which is consistent with REDD+ attenuating cross-cell spillovers through international coordination.

Contribution to the literature The paper contributes to three strands of economics literature. The paper contributes to the literature on globalization and epidemics, where existing work shows that global economic integration can propagate infectious diseases through human mobility and trade in goods (Oster, 2012; Lin et al., 2022; Antràs et al., 2023; Beverelli and Ticku, 2025). We highlight a new channel, that is, the global demand for agricultural commodities induces change in land use, which in turn creates ecological and market conditions that accelerate the spread of animal diseases and occasionally spill over to humans.

The paper also contributes to the literature documenting the externalities of land-use. Large-scale deforestation has been shown to affect rainfall, agricultural productivity, and human

health (Leite-Filho et al., 2021; de Souza Batista et al., 2023; Berazneva and Byker, 2017, 2024; Cordoba, 2024). The impact of deforestation on biodiversity remains underexplored.[1] We make progress in this direction by showing that deforestation generates a novel externality through the spread of infectious diseases among animals. This highlights a previously underexplored cost of land-use change in form of biodiversity loss.

Finally, the paper relates to the literature connecting market forces to natural resource depletion. The economics literature links weak property rights, competition, and trade-fueled demand to the overexploitation of animal resources (Allen and Keay, 2004; Carlos and Lewis, 1993; Taylor, 2011). We identify a distinct pathway: destruction of forest land for agricultural expansion indirectly spreads diseases across animal populations. This mechanism ties global commodity markets to hidden health risks, thus reframing deforestation as not only an environmental concern but also a cross-sectoral economic externality.

2 Data

We collect data on deforestation, animal disease, and several control variables at the level of grid cells – square polygons of size $\sim 0.5° \times 0.5°$ ($\sim$ 50–55 km at the Equator) – over the period 2004-2018. This section describes key data and their sources.

Deforestation. We use tropical deforestation data from Berman et al. (2023), based on the methodology developed by Hansen et al. (2010). Their dataset covers grid cells located between the Tropic of Cancer and the Tropic of Capricorn for the period 2001-2018. Deforestation at the cell level is defined as the number of pixels, which are spatial units of approximately 30 meters, within grid cell c where the pixel must satisfy two conditions to be considered deforested: (i) it had at least 50% forest cover (vegetation taller than 5 meters) in the year 2000, and (ii) it experienced a complete removal of forest cover in year t (for $t \geq 2004$).[2]

Our baseline measure of deforestation is computed across the cells that are neighbours, i.e. adjacent to grid cell c. The baseline measure of deforestation in neighbouring cells is the total, year-specific forest cover loss across all pixels with forest cover of at least 50% in 2000 in cells adjacent to cell c, i.e. those indicated as NW, N, NE, E, SE, S, SW, and W neighbouring cell in the stylized graphical representation in Figure 1. For consistency in measuring neighbourhood

[1] A recent VoxDev literature review on deforestation notes that forest "conservation has important benefits for biodiversity, even as current work typically focuses on carbon emissions. The difficulty lies in quantifying the economic gains from biodiversity, but the first step is to quantify impacts on biodiversity itself.". VoxDev Lit, Deforestation (23.09.25). https://voxdev.org/voxdevlit/deforestation.

[2] Each cell includes 4 million pixels. In robustness exercises, we modify criterion (i), alternately identifying pixels with a threshold of at least 25% of forest cover in 2000. Note that the dataset does not include partial removal of forest cover, i.e. forest degradation, in the definition of deforestation.

Figure 1: Illustration of the neigbouring cells deforestation variable

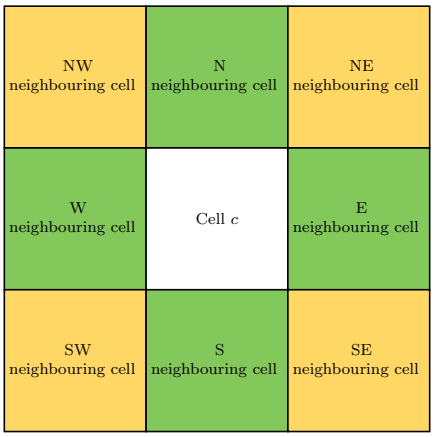

Notes: The figure visualizes how we calculate our main explanatory variable. For a target cell c, we compute the total number of pixels lost to deforestation across all neighbouring cells ($j \in \mathcal{N}(c)$; $\mathcal{N}(c) = \text{NW}, \text{N}, \text{NE}, \text{E}, \text{SE}, \text{S}, \text{SW}, \text{W}, \text{NW}$) in a year. Deforestation data, based on Hansen et al. (2010)'s methodology, are from Berman et al. (2023).

deforestation, we restrict the sample to those tropical cells that have a full neighbourhood of eight cells. This drops about 15% of cells that are mostly coastal.

While the immediate eight-neighbour measure is intuitive, it imposes two limitations for our setting. First, it equally weights all adjacent cells and ignores slightly more distant locations, even though ecological and trade processes operate over continuous space rather than administrative adjacency. Second, with 0.5 degree × 0.5 degree grid cells, the adjacency definition involves a narrow buffer around a cell and may understate the spatial reach of spillovers. To address these concerns, and to quantify the radius over which deforestation matters, we complement the adjacency measure with a distance-based neighbourhood constructed in concentric rings around each cell. The alternative methodology produces exposures that vary smoothly with distance and reduces sensitivity to arbitrarily chosen contiguity.

Animal diseases. We rely on the FAO EMPRES-i dataset, which records approximately 95,000 outbreaks of 31 diseases with confirmed cases across 174 countries between 2004 and 2020. The data include: (i) the type of disease recorded, (ii) the event date, description, and impact (number of infected animals), and (iii) the geographical coordinates (latitude and longitude) of the outbreak. The event description allows us to characterize the type(s) of animals affected, i.e. whether they are domestic, and therefore are in Harmonized System (HS) headings 0101-0105, or wild (HS heading 0106).[3] We further use these descriptions to determine whether affected wild animals are in their natural habitat or are captive-bred. If the latter, we classify them with domestic animals. This reclassification is important because our

[3]HS 0101 includes "Horses, hinnies and donkeys"; 0102 includes "Bovine animals"; 0103 includes "Swine"; 0104 includes "Sheep and goats"; 0105 includes "Poultry"; 0106 comprises of "Other live animals".

analysis focuses on deforestation-driven habitat disruptions, which are most relevant for wild animals living in their natural environments, not those in captivity. Finally, the geographical coordinates allow us to geolocate each event and assign it to a given cell. Aggregating across all events that took place within a cell in a year, we are therefore able to obtain a dataset with the overall number of infected animals, as well as the number of infected domestic (including captive) and/or wild animals, per cell c in year t. The EMPRES-i dataset also identifies rare instances of animal diseases spreading to humans (zoonotic transmissions). We use these data to conduct an exploratory analysis on how deforestation can impact human health.

Other variables. We collect additional data to capture relevant time-varying characteristics of a grid cell. These include livestock population, sourced from Du et al. (2025);[4] conflict-related fatalities, sourced from the Uppsala Conflict Data Program's Georeferenced Event Dataset Global version 25.1 (Sundberg and Melander, 2013; Pettersson and Öberg, 2020), which indicate the socio-political climate; annual average temperature and precipitation, sourced from Berman et al. (2023), which proxy the local micro-climate; measures of economic activity using nightlights data, sourced from Li et al. (2020); and human population data sourced from Liu et al. (2024).[5] In addition to the time-varying controls we collect cross-sectional data on road density (meters of road per square km) from Meijer et al. (2018), which we use to proxy market access.[6] We also collect time-varying country-level data on the number of screening and surveillance measures implemented by countries to regulate the spread of animal diseases. Screening measures are diagnostic tests carried out systematically either to regulate a specific animal disease, or to qualify herds/flocks as free from the disease. Surveillance measures continuously investigate a given population to detect the occurrence of disease for control purposes, and it might involve testing a part of the population. The data are collected from Beverelli and Ticku (2025), based on raw information provided by World Organisation for Animal Health (formerly OIE).

The final dataset includes 12,295 cells in 93 tropical countries between 2004 and 2018, while the estimation sample includes up to 60 countries and 1,083 cells over the same period. This difference is explained: (i) by us excluding the 1,768 cells with less than eight neigbouring cells

[4]The raw data reflect average animal density, in heads per square kilometer, at a spatial resolution of $\sim 5 \times 5$ km, for the following categories of animals: buffaloes, cattle, chicken, ducks, goats, horses, pigs, and sheep. Based on these raw data, we compute an approximate cell-level headcount as density × area.

[5]The raw data in Li et al. (2020) and in Liu et al. (2024) are at a 30 arc-seconds resolution ($\sim 1 \times 1$ km).

[6]The raw data are from the GRIP4 global density raster, combining all types of roads (highways primary, secondary, tertiary, and local roads) at a 5 arc minutes resolution ($\sim 8 \times 8$ km). These data do not have time variation. As explained by Meijer et al. (2018), over 50% of the road length included in GRIP4 is from data sources published in 2010 or later. A further 23% is from data sources published between 2006 and 2010, 14% was published between 2000 and 2005, and 8% is based on the VMAP0 data, covering 1979-1997.

Figure 2: Diseases and deforestation in the Tropics

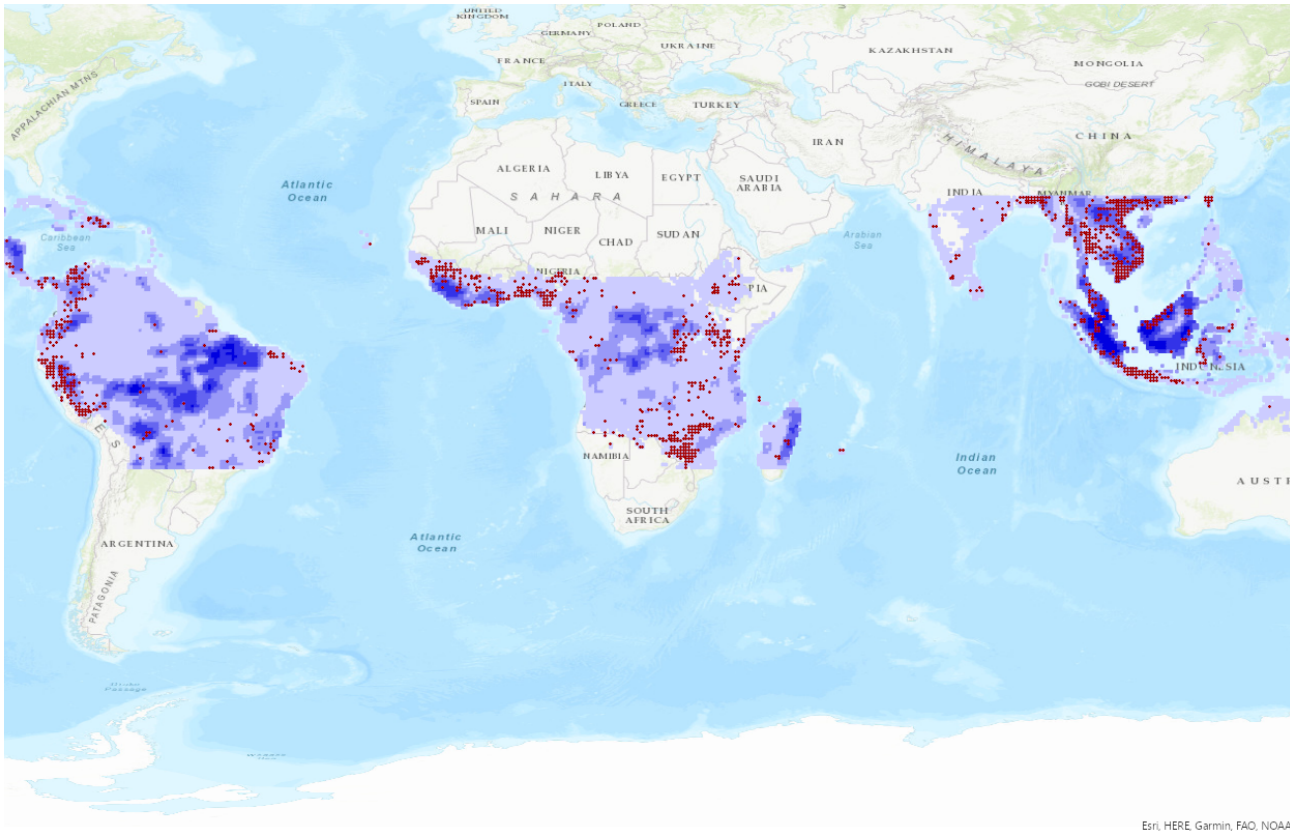

Notes: The coloured part of the world map covers the Tropics, for which we have both deforestation and animal diseases data. Total deforestation is summed between 2004 and 2018 in cells neighbouring cell c. The graduated colours identify the intensity of neighbourhood deforestation for each cell c. Red dots identify cells where at least one disease outbreak was identified during the sample period. Deforestation data, based on Hansen et al. (2010)'s methodology, are sourced from Berman et al. (2023). Disease outbreak data are from FAO EMPRES-i (see Beverelli and Ticku, 2025 for details).

from the set of 12,295 cells; and (ii) by the estimator automatically excluding those cells that did not experience any disease outbreak during the 2004-2018 period, for reasons explained in the paragraph below. Appendix Table A.1 provides summary statistics from the estimation sample for all variables included in the empirical analysis.

Figure 2 presents our baseline measure of deforestation in neighbouring grid cells, aggregated over the 2004–2018 period. It also highlights the locations that experienced at least one animal disease outbreak during this period of time. The figure illustrates that such outbreaks are relatively rare: the majority of grid cells did not report any disease event over the 15-year period. Out of the 10,537 tropical grid cells with eight neighbours in the sample, 1,083 (10.3%) recorded at least one outbreak. Our empirical analysis uses a PPML estimator with cell and year fixed effects on the tropical cell $\times$ year panel for all grid cells that have eight first-order neighbours (animal infections are set to zero when no outbreak is recorded). Under PPML with cell fixed effects, any cell with infections equal to zero in all years is perfectly separated and therefore dropped automatically by the estimator; the identification thus comes from cells with at least one recorded outbreak.

3 Empirical strategy

3.1 Baseline specification

The empirical specification estimating the impact of neighbourhood deforestation on the spread of infectious animal diseases takes the following form:

$$Infections_{ct} = \exp\left(\beta Deforestation_{ct}^{Neighbour} + \boldsymbol{\gamma}'\mathbf{z}_{ct} + \lambda_c + \mu_t\right) + \varepsilon_{ct} \tag{1}$$

where the dependent variable, $Infections_{ct}$ is defined as the total number of infection cases specific to live animals during year t in cell c. The model is estimated using Poisson Pseudo Maximum Likelihood (PPML), which is identical to a fixed effects Poisson model, but can also deal with clustered standard errors. Standard errors are clustered within a cell, but we perform a series of robustness checks to address the possibility that standard errors might exhibit spatial or serial correlation.[7] Another advantage of the PPML estimator is that it provides a natural way to deal with zeroes in the dependent variable (Santos Silva and Tenreyro, 2006).[8]

The explanatory variable of interest, $Deforestation_{ct}^{Neighbour}$, is calculated by summing the total number of pixels lost to deforestation in cell c's neighbouring cells (see Figure 1) in year t. The neighbourhood deforestation measure is expressed as logs in the baseline analysis. The coefficient of interest β measures the percentage change in animal infection cases that corresponds to a one percent increase in total deforestation in the neighbourhood. A positive coefficient would be consistent with our hypothesis that neigbourhood deforestation causes the spread of infectious animal diseases. $\mathbf{z}_{ct}$ is a vector of cell-level controls that might be associated with the spread of infectious animal diseases in the same cell. λ_i and μ_t correspond to cell and year fixed effects. All regressions are run on the full tropical grid restricted to cells with eight neighbours; PPML with cell fixed effects automatically omits always-zero cells due to separation.

Identifying assumptions. Our interpretation of β being a causal estimate rests on the assumption that the explanatory variable is potentially exogenous to any omitted factors within a target cell that might be correlated with the spread of animal diseases. We test the sensitivity

[7] In a robustness exercise discussed in Appendix Table A.4, we cluster standard errors at the province as well as at the country level to address the possibility that errors might be spatially correlated over large geographical units. In another robustness check, we cluster standard errors by cell and by year to also account for serial correlation across years. Another robustness exercise reported in Appendix Table A.5 allows errors to be spatially correlated at different distance cutoffs.

[8] In the baseline regression of column 1 of Table 1, out of 16,245 observations, the dependent variable has 14,357 zeros and 1,888 positive values. See the last two columns of Appendix Table A.1.

of our results to a variety of methodological choices – directly controlling for deforestation in the target cell, as well as including additional cell-level controls which proxy local livestock population, environmental conditions, socio-political climate and economic activity. Additionally, we control for country-year fixed effects to address concern that evolving agricultural patterns or technological changes across countries might affect both neighbourhood deforestation and infectious animal diseases. We go a step further and control for province-year fixed effects that account for any local variation in these dynamics. Yet another concern is that countries might differ in their surveillance capacities that might be correlated with deforestation incentives, which will generate a reporting bias. We address this concern by including the number of animal disease screening and surveillance measures that countries implement over time, thus accounting for reporting differences that might bias our results.

4 Results

Baseline results. Table 1 presents the baseline findings. The point estimate from column 1, with the inclusion of cell and year fixed effects, suggests that a one-percent rise in neighbourhood deforestation leads to a 1.6% increase in animal infections, with a 95 percent confidence interval of 0.9–2.2%. Using the estimated elasticity and the sample means, a 1,000-hectare increase in neighbouring deforestation implies roughly 161 additional infected animals.[9] The results are robust to the inclusion of country-year fixed effects in column 2, to controlling for own deforestation (also expressed in logs) in column 3 alongwith country-year fixed effects in column 4, and to the inclusion of various time-varying controls that capture cell-specific livestock and human populations, socio-political dynamics, local micro-climate, and the economic activity in column 5, alongside country-year fixed effects in column 6. Across all these specifications, the elasticity of animal infections to neighbourhood deforestation ranges from 1.6 to 1.8. Column 7 is presented with the addition of province-year fixed effects. Even in this demanding specification, where we lose three-fifths of the sample, neighbouring deforestation continues to have robust and economically significant effect on the spread of infectious diseases in a cell. Finally, in column 8 we include country specific measures of animal diseases surveillance and screening that varies overtime, and show that the results are robust to controlling for reporting differences across countries.

Distance-based neighbourhood exposure. Going beyond adjacency and to quantify the spatial reach of spillovers, we re-define neighbourhood deforestation using concentric distance

[9]Estimation sample mean infections = 834 infected animals; mean neighbouring deforestation = 91,937 pixels, with 1 pixel = 0.09 ha. ΔInfections = $\beta \times \left(\frac{1000}{\text{Mean Deforestation (ha)}}\right) \times$ Mean Infections.

Table 1: Deforestation and diseases: Baseline results

VARIABLES	(1)	(2)	(3)	(4)	(5)	(6)	(7)	(8)
	sumcases_overall							
Neighbouring deforestation	1.56***	1.66**	1.65***	1.84**	1.72***	1.56**	0.71**	1.72***
	(0.34)	(0.75)	(0.31)	(0.74)	(0.37)	(0.63)	(0.35)	(0.37)
Own deforestation			-0.14	-0.33	-0.17	-0.23	-0.10	-0.16
			(0.16)	(0.21)	(0.12)	(0.16)	(0.26)	(0.12)
Livestock headcount					1.70**	1.01***	-0.51	1.54*
					(0.81)	(0.35)	(0.67)	(0.84)
Conflict fatalities					-0.15	-0.07	-0.10	-0.15
					(0.15)	(0.05)	(0.14)	(0.15)
Temperature					2.93***	-5.73**	-9.66	2.62***
					(0.74)	(2.49)	(12.36)	(0.69)
Precipitation					-0.00**	-0.00	-0.00	-0.00***
					(0.00)	(0.00)	(0.00)	(0.00)
Population					5.20**	1.37	3.67	4.22*
					(2.18)	(1.34)	(3.41)	(2.17)
Nightlights					-0.54***	-0.17	-0.16	-0.48***
					(0.11)	(0.12)	(0.19)	(0.11)
Screenings								0.02
								(0.08)
Surveillances								-0.13**
								(0.05)
Cell FE	Yes	Yes	Yes	Yes	Yes	Yes	Yes	Yes
Year FE	Yes	No	Yes	No	Yes	No	No	Yes
Country × Year FE	No	Yes	No	Yes	No	Yes	No	No
Province × Year FE	No	No	No	No	No	No	Yes	No
No. of countries	60	48	60	48	60	48	38	60
No. of years	15	15	15	15	15	15	15	15
No. of cells	1,083	1,065	1,083	1,065	1,083	1,065	788	1,083
Observations	16,245	10,180	16,245	10,180	16,245	10,180	3,727	16,245

Notes: *** $p < 0.01$, ** $p < 0.05$, * $p < 0.1$. Dependent variable: Number of animal infection cases in cell c in year t. Years: 2004–2018. Standard errors clustered by cell in parentheses. See Section 2 and Table A.1 for variable definitions.

rings around each cell's centroid. For each cell c and year t we compute the sum of deforestation in (i) 0–100 km, (ii) 100–250 km, and (iii) 250–500 km rings, excluding own-cell deforestation. We then estimate a PPML model with cell and year fixed effects, and own cell controls, akin to column 5 of Table 1:

$$\begin{aligned} \mathit{Infections}_{ct} = \exp\Big(& \beta_{0\text{–}100}\,\mathrm{DeforestationNeighbour}_{ct}^{0\text{–}100} + \beta_{100\text{–}250}\,\mathrm{DeforestationNeighbour}_{ct}^{100\text{–}250} \\ & + \beta_{250\text{–}500}\,\mathrm{DeforestationNeighbour}_{ct}^{250\text{–}500} + \boldsymbol{\gamma}'\mathbf{z}_{ct} + \lambda_c + \mu_t \Big) + \varepsilon_{ct}. \end{aligned} \tag{2}$$

Figure 3 plots the estimates from equation (2). The results indicate that deforestation within 0–100 km significantly raises animal infections. The coefficient for remote distance rings are negative and statistically significant, but this pattern does not persist when using finer distance bins (Appendix Figure A.9). We therefore view this as likely reflecting noise or aggregation

Figure 3: Distance-based deforestation exposure

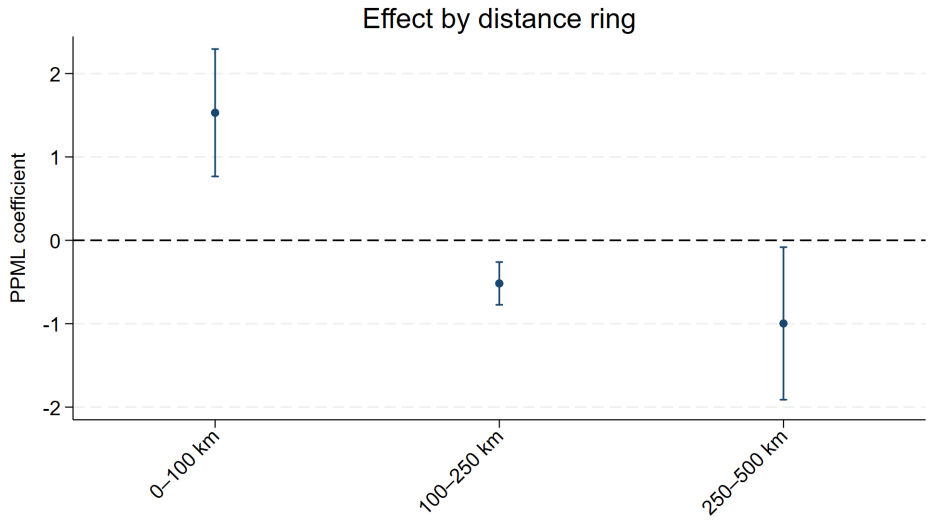

Notes: Dependent variable: Number of animal infection cases in cell c in year t. Years: 2004–2018. Standard errors clustered by cell in parentheses. 95% confidence intervals are reported by the vertical bars.

across heterogeneous distances, rather than a genuine dampening effect. Overall, the evidence indicates that spillover effects of deforestation are highly localized.

Additional robustness checks. We conduct a series of robustness checks on the results of column 5 of Table 1, which are described in Appendix Section A.4 and reported in Appendix Tables A.4 and A.5. We show that the results are robust to alternative definitions of the deforestation variable, exclusion of the first year in the sample (2004), which was an outlier in terms of recorded infections, as well as excluding outlier epidemics across years, exclusion of zeros in the construction of the dependent variable, and alternative clustering of standard errors, which includes clustering on distance-based blocks to allow for spatially correlated inference. Together, these results confirm that neighbourhood deforestation has a robust positive effect on the spread of infectious animal diseases.

Quantification. We estimate country-specific elasticities from the specification in Column (1) in Table 1, where the neighbourhood deforestation variable is also interacted with country dummies, and translate the coefficients into absolute changes in animal infections per 1,000 hectares of deforestation.[10] The estimated infection counts are calculated by combining each country's elasticity with its own mean infection level and mean neighbouring deforestation (in hectares). The quantification exercise highlights striking cross-country heterogeneity. The top ten most affected countries are shown in Figure 4. Mexico and Taiwan stand out with

[10]Note that standard errors on country-specific coefficients (β_c) are not estimated when we include own-cell controls, as in Column (5). So we compute the elasticities from Column (1) of Table 1, with only cell and year fixed effects.

Figure 4: Quantification: Deforestation and animal infections

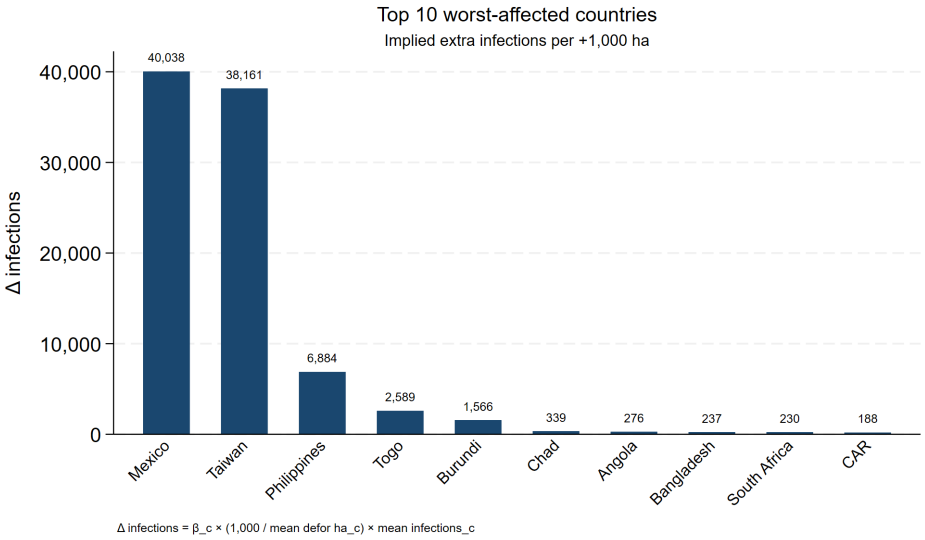

Notes: The bar graph is based on country-specific elasticities that are estimated from the specification in Column (1) in Table 1, where the neighbourhood deforestation variable is interacted with country dummies.

particularly large magnitudes: an additional 1,000 hectares of deforestation is associated with approximately 40,000 extra animal infections on average. The Philippines follows with nearly 7,000 infections, while Togo and Burundi each show increases in the range of 1,500–2,600 infections. The remaining countries in the top ten (Chad, Angola, Bangladesh, South Africa, and the Central African Republic) exhibit smaller, though non-trivial, impacts. These results underscore that the disease burden of deforestation is highly concentrated: in some countries deforestation translates into tens of thousands of additional animal infections, while in others the effects are much smaller.

Instrumental variable design. To further strengthen the causal interpretation, we exploit the increases in international crop prices that raise demand for agricultural land, and therefore deforestation (Berman et al., 2023), in neighbouring cells. Specifically, we use an IV design in which we isolate the change in deforestation that is due to a change in the price index of crops across neighbouring cells, in order to identify its causal effect on the spread of animal diseases in a target cell. The first stage of the IV model takes the following form:

$$Deforestation_{ct}^{Neighbour} = \alpha PriceIndex_{ct}^{Neighbour} + \lambda_i + \mu_t + v_{ct} \tag{3}$$

where the instrument, $PriceIndex_{ct}^{Neighbour}$, is the average of the crop price index of cells in the neighbourhood of cell c in year t. The data on crop price index are taken from Berman et al. (2023), who collect data on 15 crops traded on international markets for which annual global

price data and agronomic suitability data are available. For each cell c and year t, the crop price index is calculated as a weighted sum of the annual price of each crop, with weights given by the cell-specific relative suitability of each crop.[11] Both the measures of deforestation and the average crop index are expressed in logs.

The second stage takes the following form:

$$Infections_{ct} = \exp\left(\beta^{IV} Deforestation_{ct}^{Neighbour} + \lambda_c + \mu_t\right) + u_{ct} \tag{4}$$

The IV regression is estimated using an instrumental variable methodology suitable for exponential regressions with two-way fixed effects (Jochmans and Verardi, 2022).

Table 2 presents the results from the IV-PPML model with two-way fixed effects (equation (4)). In this specification, the elasticity of animal infections to neighbourhood infections is about 1.3 and the effect is statistically significant at 1 percent level. We additionally present the first-stage results, estimated through a linear regression of neighborhood deforestation on the instrument, controlling for cell and year fixed effects. The instrument's relevance is confirmed by the Kleibergen–Paap F-statistic being 13, which exceeds the conventional threshold of 10 used to flag weak instruments. Overall, the results of the IV estimation bolster the internal validity of our findings.[12]

Our IV's validity rests on the assumption that the rise in international crop prices accelerates neighbourhood deforestation by raising demand for cropland. We put the validity of our instrument to test by building a *placebo* instrument, $PriceIndex_{ct}^{Neighbour,5-least}$, that is the average of the price index of 5 least suitable crops for each neighbouring cell of cell c in year t. If international crop prices impact animal infections solely through neighbourhood deforestation, that is induced by higher demand for cropland, we should expect the placebo IV to have a null effect on both neighbourhood deforestation and infection cases. Appendix Table A.3 shows that the placebo IV is neither correlated with neighbourhood deforestation, nor does it impact infection cases in a cell in year. When they are not anticipated to raise agricultural demand, international crop prices neither impact neighbourhood deforestation nor they are related to

[11] Relative suitability is calculated by Berman et al. (2023) as follows: agronomic suitability is defined as the percentage of the maximum yield that can be attained in each grid cell. Relative suitability is calculated by dividing the suitability of the crop by the sum of the suitability of all crops. The 15 crops used to calculate the measure are bananas, barley, cocoa, coconuts, coffee, cotton, maize, palm oil, rice, sorghum, soybeans, sugar, tea, tobacco, and wheat.

[12] We also estimated IV-PPML regressions adding own deforestation, instrumented using the own crop price index. The results, available upon request, are quantitatively similar to the corresponding PPML results of column 3 of Table 1. For technical reasons due to lack of convergence, IV-PPML regressions could not be estimated adding additional controls or country-year fixed effects.

Table 2: Deforestation and diseases: IV results

VARIABLES	(1) First stage	(2) Second stage (IV-PPML)
Neighbouring price index	0.60***	
	(0.17)	
Neighbouring deforestation		1.27***
		(0.19)
Cell FE	Yes	Yes
Year FE	Yes	Yes
Country × Year FE	No	No
KP F-statistic	12.50	
No. of countries	60	60
No. of years	15	15
No. of cells	1,083	1,083
Observations	16,245	16,245

Notes: *** $p < 0.01$, ** $p < 0.05$, * $p < 0.1$. Column (1) reports the first-stage regression of the endogenous regressor on the excluded instrument. Column (2) reports second-stage estimates from an IV estimator of exponential regression models with two-way fixed effects. Years: 2004–2018. Standard errors clustered by cell in parentheses. Estimation is implemented in `Stata` using the `ivgravity` package (Jochmans and Verardi, 2022). See Section 2 and Table A.1 for variable definitions.

animal infections. This bolsters the internal validity of our instrument.

5 Mechanisms: Wildlife habitat destruction vs. market access

There are two potential mechanisms through which nearby deforestation can contribute to the spread of infectious animal diseases in a location. Firstly, loss of wildlife habitat induced by deforestation can amplify the interaction between wildlife and domesticated animals. The increase in contact between wildlife species, that are reservoirs of various pathogens, and domesticated species can result in the spread of infectious diseases among domesticated animals (Dobson et al., 2020). Deforestation-driven contact between wildlife and domestic animals is highlighted by Faust et al. (2018), who estimate that wildlife species are most likely to interact with livestock and humans when more than 25% of the original forest cover is lost. Numerous studies also pinpoint the exact mechanism through which deforestation-related disturbance results in transmission of novel pathogens from wildlife species to domestic animals. For instance, Jones et al. (2024) find a positive association between deforestation and incidents of bovine rabies outbreaks in Costa Rica, which are initiated by vampire bats transmitting the rabies virus to cattle. The emergence of bat-associated viruses in Australia is attributed to deforestation and agricultural expansion, causing bats to forage in periurban fruit trees, increasing their interaction with livestock and humans, thus increasing the likelihood of pathogen spillover (Jones et al., 2013). Sehgal (2010) argues that deforestation can alter the flight pathways and increase contact between different avian populations, potentially resulting in the spread of avian

Figure 5: Neighbourhood deforestation and infectious animal diseases

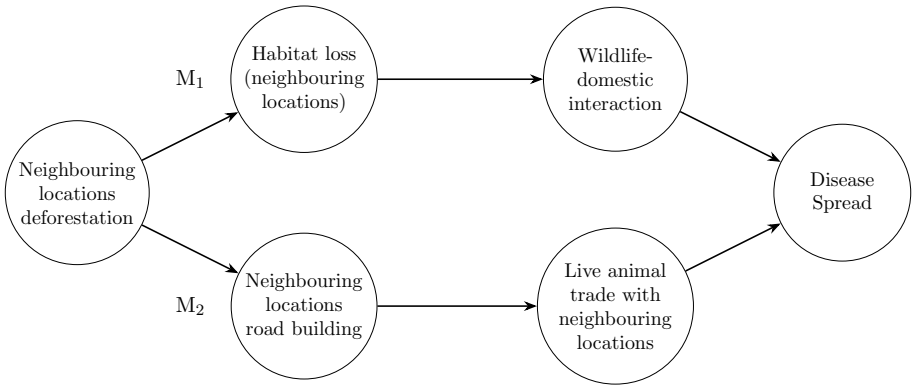

Notes: The figure visualizes the two mechanisms – wildlife habitat destruction (M_1) and trade-related contagion (M_1) – through which the spread of infectious animal diseases in a given location can be driven by deforestation in neighbouring locations.

influenza.

A second possibility is that deforestation-related road construction facilitates animal trade with neigbouring locations.[13] The heightened movement of animals through trade can then amplify the likelihood of contagion (Ticku and Beverelli, 2023).

Figure 5 highlights these two distinct mechanisms through which deforestation in the neighbourhood can result in the spread of infectious animal diseases.

To investigate the role of habitat destruction in the relationship between deforestation and disease outbreaks, we adopt two approaches. First, we focus on the eight diseases in the FAO EMPRES-i database known to affect both wildlife and domestic species. These include African swine fever, Anthrax, Classical swine fever, Avian influenza, Newcastle disease, Rabies, Rift Valley fever, and West Nile fever.[14] Column (1) of Table 3 shows that the effect of deforestation in neighbouring cells remains virtually unchanged when the analysis is restricted to this subset of diseases. This finding suggests that neighbourhood deforestation has a particularly strong impact on diseases that cross the wildlife–livestock interface, providing *prima facie* evidence that increased contact between wild and domesticated animals – plausibly driven by habitat loss – plays a role in disease transmission.

In a related test, we examine whether the effect of neighbourhood deforestation is particularly pronounced when nearby cells also report infectious disease cases among wild animals. A

[13]It is also possible that road construction leads to deforestation (Pfaff et al., 2007; Asher et al., 2020). In that instance too, deforestation captures the market access mechanism that we are interested in.

[14]These diseases were identified through textual analysis of the species descriptions associated with each outbreak. Domestic animals also include captive species.

heightened effect if there are instances of infections among wildlife in neigbouring cells would be consistent with the hypothesis that deforestation prompts the movement of infected wildlife from neigbouring cells, thereby increasing the risk of transmission to domesticated animals. Column (2) of Table 3 reports results from a specification in which the dependent variable includes only cases affecting domestic animals. The key explanatory variable is the interaction between neighbourhood deforestation and the variable wildlife cases – a binary indicator that equals one if at least one wildlife infection is recorded in the neighbouring cells. The findings indicate that neighbourhood deforestation results in the spread of infectious diseases among domestic animals only when wildlife infections are also present in the same vicinity – supporting the idea that deforestation-driven contact between wildlife and livestock plays a critical role in disease spread.

Next, we examine whether deforestation in neighbouring areas increases infectious animal diseases by improving market access and facilitating greater movement of live animals through trade. To test this mechanism, Column (3) of Table 3 includes an interaction between time-varying deforestation in neighbouring cells and a time-invariant dummy for road density in those cells. The dummy equals one if road density (measured in meters per square kilometer) in cell c's neighbourhood is above the median road density observed across the 1,083 cells included in the sample of column 1 of Table 1.[15] The road density dummy captures baseline differences in neighbourhood connectivity, while deforestation captures time-varying changes in market access in the neighbourhood. A positive coefficient on the interaction term would indicate that the effect of deforestation is amplified in cells with better neighbourhood connectivity, consistent with increased trade driving the spread of animal disease. Indeed, the positive and statistically significant interaction in column 3 supports this trade-based explanation.

Finally, in column 4 of Table 3 we run a horse-race between the wildlife habitat destruction and market access mechanisms. Both interaction terms continue to be statistically significant, and therefore suggest that both channels are empirically relevant. However, the effect of wildlife habitat destruction is approximately three times that of the trade related channel, indicating that the former channel is quantitatively more relevant.

[15]The dependent variable in column 3 of Table 3 includes only cases involving domestic or captive animals. Although the trade mechanism – linked to road infrastructure – does not require excluding wildlife cases, focusing on domestic/captive animals allows comparability across mechanisms. Notably, results remain unchanged if all cases (including wildlife) are used; these are available upon request.

Table 3: Deforestation and diseases: Mechanisms

Dependent variable	Cases in eight diseases	Cases affecting domestic		
	(1)	(2)	(3)	(4)
Neighbouring cells deforestation	1.86***	0.46	0.11	-0.03
	(0.40)	(0.31)	(0.27)	(0.25)
Neighbouring cells wildlife cases		-28.28***		-25.51***
		(8.97)		(8.68)
Neighbouring cells (deforestation × wildlife cases)		2.81***		2.54***
		(0.80)		(0.77)
Neighbouring cells (deforestation × road density)			0.97***	0.72***
			(0.30)	(0.26)
Cell FE	Yes	Yes	Yes	Yes
Year FE	Yes	Yes	Yes	Yes
Own cell controls	Yes	Yes	Yes	Yes
No. of cells	691	940	940	940
No. of countries	47	58	58	58
Observations	10,365	14,100	14,100	14,100

Notes: *** $p < 0.01$, ** $p < 0.05$, * $p < 0.1$. PPML regressions. Dependent variable in column 1: Number of animal infection cases in cell c in year t, summed across all outbreaks within the eight diseases where wild-domestic/captive interaction is recorded (African swine fever; Anthrax; Classical swine fever; Avian influenza; Newcastle disease; Rabies; Rift Valley fever; West Nile Fever). Dependent variable in columns (2)–(4): Number of animal infection cases in cell c in year t, summed across all outbreaks including domestic/captive animals in HS headings 0101–0105 (and excluding wildlife). The variable wildlife cases is a dummy equal to one if at least one wildlife infection is recorded in cell c's neighbourhood. The variable road density is a dummy equal to one if road density (measured in meters per square kilometer) in cell c's neighbourhood is above the median road density observed across the 1,083 cells included in the sample of column 1 of Table 1. Own cell controls: own deforestation, livestock headcount, conflict fatalities, temperature, rainfall, population, and nightlights. Years: 2004–2018. See Section 2 and Table A.1 for variables' description.

6 Event study analysis

Our baseline analysis quantifies the average contemporaneous effect of neighbourhood deforestation on the spread infectious animal diseases. This section provides a complementary analysis where we identify the dynamic effects of sharp deforestation shocks in the neighbourhood. For each cell, we determine the shock to be the strongest year-on-year increase in neighbourhood deforestation,[16] conditional on the change being in the top 10 percentile of the overall sample, to focus on economically meaningful changes.[17] We regress the outcome variable on dummies corresponding to the years before, at the time of, and years after the neighbourhood shock to identify the dynamics of the infections spread around a large spike in neighbourhood deforestation.

We estimate the following event study with PPML:

$$Infections_{ct} = \exp\left(\sum_{k=-5,\, k\neq -1}^{5} \beta_k \, D_{ct}^{k} \; + \; \boldsymbol{\gamma}' \mathbf{z}_{ct} \; + \; \lambda_c \; + \; \mu_t \right) + \varepsilon_{ct}. \tag{5}$$

[16] In case of multiple year-on-year increases that are the same, we consider the earliest year as the treatment year.

[17] Event study results with alternative threshold of top 5 percentile changes of the overall sample are shown in the Appendix Section A.5, and they reveal a similar pattern.

Figure 6: Neighbourhood deforestation spikes and diseases

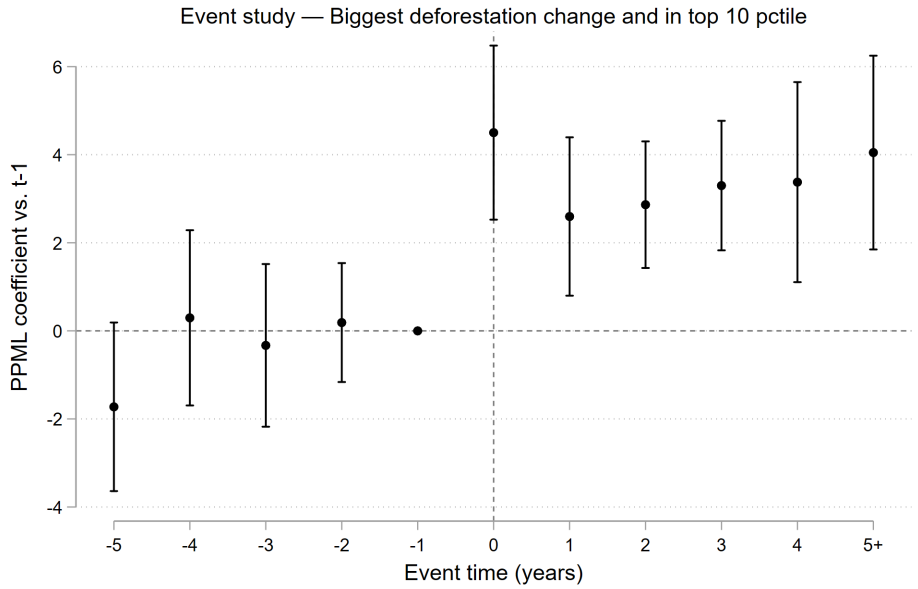

Notes: The figure showcases the dynamics of animal infections around the time of a large deforestation spike in the neighbourhood, as detailed in equation 5. Cell and year fixed effect, along with own-cell controls are included in the estimation. 95% confidence intervals are reported by the vertical bars. Event time -1 is set as the reference period and hence not included in the estimation.

Here $\tau_{ct} = t - T_c^*$ is event time, with T_c^* the event year defined by the strongest neighbouring-deforestation spike; D_{ct}^k is a dummy that equals 1 when $\tau_{ct} = k$ and 0 otherwise, for $k \in \{-5, -4, -3, -2, 0, 1, 2, 3, 4, 5\}$ and with $k = -1$ omitted as the reference period; $\mathbf{z}_{ct}$ are controls; and λ_c and μ_t are cell and year fixed effects. The tails are binned, such that $k = -5$ corresponds to $\tau_{ct} \leq -5$ and $k = 5$ corresponds to $\tau_{ct} \geq 5$. Standard errors are clustered at the cell level.

Figure 6 shows no pre-trends in the number of animal infections prior to the neighbourhood deforestation shock and slightly delayed and persistent effect in the years since, with effects still present in the binned +5 horizon, consistent with a durable transmission response rather than a temporary surge. This dynamic pattern reinforces the baseline elasticity by revealing that large deforestation shocks in the neighbourhood not only result in higher infections in short-run but also propagate medium-run increases in infectious animal diseases, also supportive of the wildlife–livestock contact and market-access channels documented earlier.

7 Neighbourhood deforestation and zoonotic transmissions

The FAO Empres-i dataset also records animal disease events that spill over to humans, but such events are relatively rare. For instance, in the estimation sample of column 5 in Table 1, 11% of observations recorded an animal infection, while the corresponding rate of human

Figure 7: Neighbourhood deforestation spikes and zoonotic transmissions

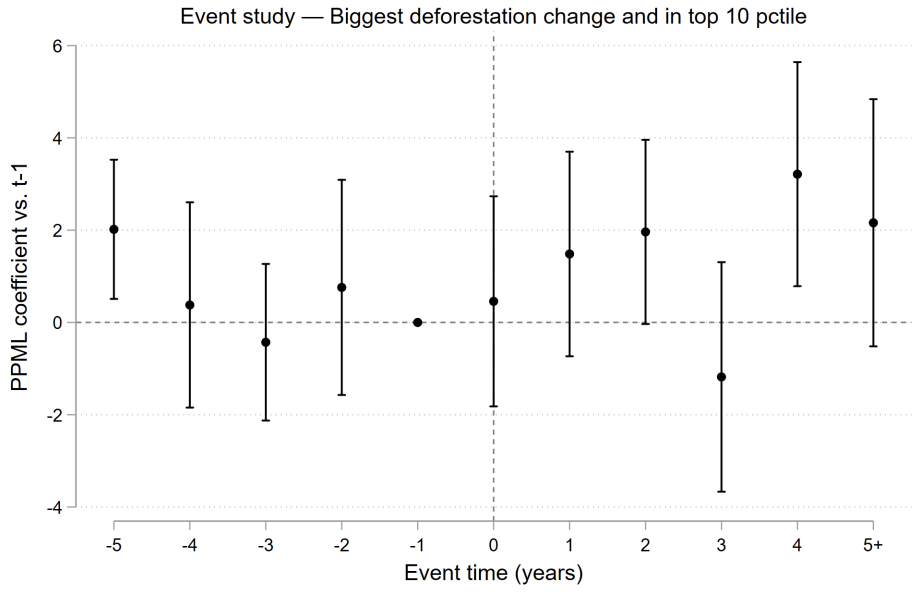

Notes: The figure showcases the dynamics of human infections around the time of a large deforestation spike in the neighbourhood, as detailed in equation 5. Cell and year fixed effects, along with own-cell controls are included in the estimation. 95% confidence intervals are reported by the vertical bars. Event time -1 is set as the reference period and hence not included in the estimation.

transmission is about 1%. With this caveat, we run the PPML specification akin to column 5 in Table 1, with the number of human infections in a cell in a year as the dependent variable. The baseline PPML estimates reveal no detectable average effect of neighbourhood deforestation (β = -0.56, p-value = 0.12). This is not surprising since confirmed zoonotic spillovers are rare in our dataset.

However, this average masks important dynamics. The annual event-study estimates presented in Figure 7 show no systematic pre-trends in human infections prior to deforestation shocks, which supports a causal interpretation. In the years following large deforestation events, point estimates suggest an increase in human infections, and the coefficients are also significant at 5 percent level in years 2 and 4.

Taken together, the results highlight the low-frequency but high-impact nature of zoonotic spillovers: most deforestation shocks do not trigger human transmission, but when they do, the resulting outbreaks can impose severe costs. From an economic perspective, this implies that the expected costs of deforestation extend beyond incremental losses in animal health and productivity. They also encompass rare but potentially catastrophic human health crises, whose social costs far exceed those borne locally.

Figure 8: Mitigation through national coordination

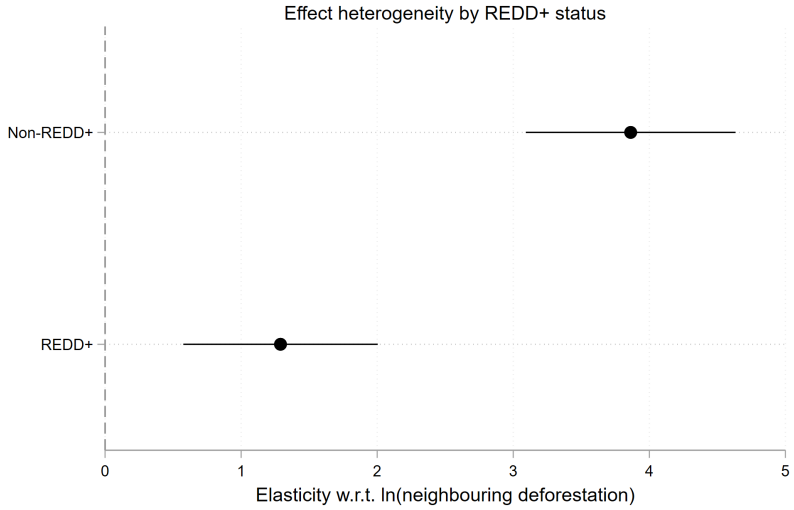

Notes: The coefficients are estimated from a model akin to column 5 of Table 1, where the neighbourhood deforestation measure is interacted with a dummy that equals 1 if a country is part of the REDD+ group.

8 Policy implication

Our central result is that deforestation generates sizable spatial spillovers in animal infections. Such externalities are unlikely to be fully internalized by local agents or subnational institutions and therefore call for coordination at the national level.

We assess one concrete coordinating device: participation in REDD+, which requires a national framework for forest governance and land-management. In our estimation sample, 51 of 60 countries are REDD+ participants, while nine are not (see Appendix Figure A.12).[18] We perform a heterogeneity analysis where we assess the differential effect of neighbourhood deforestation on animal infections across REDD+ and non-REDD+ countries. The interaction estimates presented in Figure 8 indicate that the elasticity of infections with respect to neighbouring deforestation is three times larger in non-REDD+ countries. Converting to levels at sample means, a 1,000-hectare increase in neighbouring deforestation corresponds to roughly 389 additional infected animals in non-REDD+ countries versus 130 in REDD+ countries.

These patterns are consistent with REDD+ mitigating cross-cell spillovers through national planning, land-use enforcement, and monitoring systems that can tighten controls beyond the deforesting cell. Notably, better surveillance under REDD+ could increase reported cases; observing smaller effects in REDD+ despite that possibility strengthens the interpretation that risk itself is reduced.

[18] Information on REDD+ membership is sourced from https://redd.unfccc.int/.

9 Conclusion

This paper provides causal evidence that deforestation in tropical regions contributes significantly to the spread of infectious animal diseases. Using a geo-referenced panel of disease outbreaks and forest loss data across 60 countries from 2004 to 2018, we show that deforestation in neighbouring areas results in the spread of infectious animal diseases. A simple quantification highlights substantial heterogeneity: in countries such as Mexico and Taiwan, comparable deforestation translates into tens of thousands of additional animal infections, whereas the effects are much smaller elsewhere.

We identify two main channels through which deforestation drives disease transmission: (i) habitat loss that increases contact between wildlife and domestic animals, and (ii) improved market access from road construction that facilitates the spread of livestock-borne diseases. Both channels are empirically relevant, though habitat destruction appears to play a larger role. Large deforestation shocks are also occasionally followed by significant increases in human infections.

Our findings have direct implications for land-use governance, conservation, and livestock health policy. Because deforestation in one location imposes disease spillovers on neighbouring areas, particularly where road infrastructure can facilitate animal trade, the social costs of forest loss are not borne solely by the deforesting locality. This spatial externality implies that decentralized land-use decisions may lead to socially suboptimal levels of deforestation. Policies such as payments for ecosystem services (e.g., REDD+), zoning restrictions, or conservation subsidies could be calibrated to internalize these spillovers. A simple heterogeneity test shows that countries participating in REDD+ exhibit attenuated spillovers, consistent with national planning, enforcement, and monitoring systems curbing transmission risks. Another implication of our findings is that infrastructure expansion projects should be evaluated not only on economic grounds but also in terms of their potential to accelerate pathogen transmission. Coordinated regional approaches to forest conservation and live animal trade regulation may therefore yield biosecurity benefits that are not captured by local-level incentives.

References

Allen, R. C. and I. Keay (2004): "Saving the Whales: Lessons from the Extinction of the Eastern Arctic Bowhead," *Journal of Economic History*, 64, 400–432.

Antràs, P., S. J. Redding, and E. Rossi-Hansberg (2023): "Globalization and pandemics," *American Economic Review*, 113, 939–981.

Asher, S., T. Garg, and P. Novosad (2020): "The Ecological Impact of Transportation Infrastructure," *Economic Journal*, 130, 1173–1199.

Berazneva, J. and T. S. Byker (2017): "Does Forest Loss Increase Human Disease? Evidence from Nigeria," *American Economic Review*, 107, 516–521.

——— (2024): "Impacts of Environmental Degradation: Forest Loss, Malaria, and Child Outcomes in Nigeria," *Review of Economics and Statistics*, 106, 1254–1267.

Berman, N., M. Couttenier, A. Leblois, and R. Soubeyran (2023): "Crop prices and deforestation in the tropics," *Journal of Environmental Economics and Management*, 119, 102819.

Beverelli, C. and R. Ticku (2025): "Illicit animal trade and infectious diseases," *World Development*, 191, 106969.

Carlos, A. M. and F. D. Lewis (1993): "Indians, the Beaver, and the Bay: The Economics of Depletion in the Lands of the Hudson's Bay Company, 1700–1763," *Journal of Economic History*, 53, 465–494.

Cordoba, G. F. (2024): "Deforestation and child health in Cambodia," *Economics & Human Biology*, 52, 101343.

de Souza Batista, F., C. Duku, and L. Hein (2023): "Deforestation-induced changes in rainfall decrease soybean-maize yields in Brazil," *Ecological Modelling*, 486, 110533.

Dobson, A. P., S. L. Pimm, L. Hannah, L. Kaufman, J. A. Ahumada, A. W. Ando, A. Bernstein, J. Busch, P. Daszak, J. Engelmann, M. F. Kinnaird, B. V. Li, T. Loch-Temzelides, T. Lovejoy, K. Nowak, P. R. Roehrdanz, and M. M. Vale (2020): "Ecology and economics for pandemic prevention," *Science*, 369, 379–381.

Du, Z., L. Yu, Y. Zhao, X. Li, X. Liu, X. Li, P. Hao, Z. Chen, X. Ma, and H. Wang (2025): "Annual global gridded livestock mapping from 1961 to 2021," *Earth System Science Data Discussions*, 1–20.

Faust, C. L., H. I. McCallum, L. S. Bloomfield, N. L. Gottdenker, T. R. Gillespie, C. J. Torney, A. P. Dobson, and R. K. Plowright (2018): "Pathogen spillover during land conversion," *Ecology letters*, 21, 471–483.

Hansen, M. C., S. V. Stehman, and P. V. Potapov (2010): "Quantification of global gross forest cover loss," *Proceedings of the National Academy of Sciences*, 107, 8650–8655.

Jochmans, K. and V. Verardi (2022): "Instrumental-variable estimation of exponential-regression models with two-way fixed effects with an application to gravity equations," *Journal of Applied Econometrics*, 37, 1121–1137.

Jones, B. A., D. Grace, R. Kock, S. Alonso, J. Rushton, M. Y. Said, D. McKeever, F. Mutua, J. Young, J. McDermott, and D. U. Pfeiffer (2013): "Zoonosis emergence linked to agricultural intensification and environmental change," *Proceedings of the National Academy of Sciences*, 110, 8399–8404.

Jones, C., A. Vicente-Santos, J. A. Clennon, and T. R. Gillespie (2024): "Deforestation and Bovine Rabies Outbreaks in Costa Rica, 1985–2020," *Emerging Infectious Diseases*, 30.

Leite-Filho, A. T., B. S. Soares-Filho, J. L. Davis, G. M. Abrahão, and J. Börner (2021): "Deforestation reduces rainfall and agricultural revenues in the Brazilian Amazon," *Nature Communications*, 12, 2591.

Li, X., Y. Zhou, M. Zhao, and X. Zhao (2020): "A harmonized global nighttime light dataset 1992–2018," *Scientific Data*, 7.

Lin, F., X. Wang, and M. Zhou (2022): "How trade affects pandemics? Evidence from severe acute respiratory syndromes in 2003," *The World Economy*, 45, 2270–2283.

Liu, L., X. Cao, S. Li, and N. Jie (2024): "A 31-year (1990–2020) global gridded population dataset generated by cluster analysis and statistical learning," *Scientific Data*, 11, 124.

Meijer, J. R., M. A. Huijbregts, K. C. Schotten, and A. M. Schipper (2018): "Global patterns of current and future road infrastructure," *Environmental Research Letters*, 13, 064006.

Oster, E. (2012): "Routes of Infection: Exports and Hiv Incidence in Sub-Saharan Africa," *Journal of the European Economic Association*, 10, 1025–1058.

Pettersson, T. and M. Öberg (2020): "Organized violence, 1989–2019," *Journal of Peace Research*, 57, 597–613.

Pfaff, A., J. Robalino, R. Walker, S. Aldrich, M. Caldas, E. Reis, S. Perz, C. Bohrer, E. Arima, W. Laurance, et al. (2007): "Road investments, spatial spillovers, and deforestation in the Brazilian Amazon," *Journal of Regional Science*, 47, 109–123.

Santos Silva, J. M. C. and S. Tenreyro (2006): "The Log of Gravity," *Review of Economics and Statistics*, 88, 641–658.

——— (2011): "Further simulation evidence on the performance of the Poisson pseudo-maximum likelihood estimator," *Economics Letters*, 112, 220–222.

Sehgal, R. N. M. (2010): "Deforestation and avian infectious diseases," *Journal of Experimental Biology*, 213, 955–960.

Sundberg, R. and E. Melander (2013): "Introducing the UCDP Georeferenced Event Dataset," *Journal of Peace Research*, 50, 523–532.

Taylor, M. S. (2011): "Buffalo Hunt: International Trade and the Virtual Extinction of the North American Bison," *American Economic Review*, 101, 3162–3195.

Ticku, R. and C. Beverelli (2023): "Trading Epidemics: Evidence from Eid-al-Adha," Available at https://www.researchgate.net/publication/368530367_Trading_Epidemics_Evidence_from_Eid-al-Adha.

Appendix

A.1 Variables' description and summary statistics

Table A.1: Variables' description

Variable	Description	Data source
Infection cases	Number of animals infected in grid cell c in year t.	FAO EMPRES-i
Own deforestation	Log of the number of pixels within cell c which had a forest cover of at least 50% in 2000, and that endured a loss of more than 50% of their 2000 forest cover in year t.	Berman et al. (2023)
Neighbouring cells deforestation	Log of the sum across the eight cells neighbouring cell c (see Figure 1) of their respective deforestation (ct) variable.	Authors' calculation based on raw data from Berman et al. (2023)
Livestock headcount	Log of the headcount of buffaloes, cattle, chicken, ducks, goats, horses, pigs, and sheep, computed as density × area.	Du et al. (2025)
Conflict fatalities	Sum of (most likely estimate of) total fatalities from organized violence events within cell c and year t.	UCDP GED Global version 25.1
Temperature	Average temperature, in °C, in cell c in year t.	Berman et al. (2023)
Rainfall	Average precipitations, in mm, in cell c in year t.	– ''–
Population	Human population, in log, in cell c in year t	Liu et al. (2024)
Nightlights	Average nighttime brightness intensity of cell c in year t, measured on the Defense Meteorological Satellite Program – Operational Linescan System (DMSP–OLS) 0–63 scale.	Li et al. (2020)
Price index	Log of the weighted sum of the annual average world price of crop k, weighted by the relative suitability of crop k in cell c.	Eq. (2) in Berman et al. (2023)
Neighbouring cells price index	Log of the average crop price index across cells neighbouring cell c in year t.	Authors' calculation based on raw data from Berman et al. (2023)
Neighbouring cells price index (5 least suitable crops)	Log of the average crop price index comprising 5 least suitable crops across each cell neighbouring cell c in year t.	Authors' calculation based on raw data from Berman et al. (2023)
Infection cases in eight diseases	Number of animals infected in grid cell c in year t, summed across the eight diseases known to infect both wild and domesticated animals.	FAO EMPRES-i
Neighbouring cells wildlife cases	Equals 1 if if at least one case affecting wildlife is recorded in cells neighbouring cell c in year t.	– ''–
Neighbouring cells road density	Equals 1 if if average road density (meters of road per square km) across cells neighbouring cell c is above the median road density in the 1,277 cells of column 1 of Table 1.	Authors' calculation based on raw data from Meijer et al. (2018)
Own deforestation (25)	Log of the number of pixels within cell c which had a forest cover of at least 25% in 2000, and that endured a loss of more than 50% of their 2000 forest cover in year t.	Berman et al. (2023)
Neighbouring cells deforestation (25)	Log of the sum across cells neighbouring cell c (see Figure 1) of their respective Own deforestation 25 variable.	Authors' calculation based on raw data from Berman et al. (2023)
Own deforestation (IHS)	Inverse hyperbolic sine transformation of own deforestation.	Berman et al. (2023)
Neighbouring cells deforestation (IHS)	Inverse hyperbolic sine transformation of Neighbouring cells deforestation (not in logs).	Authors' calculation based on raw data from Berman et al. (2023)
Screenings	Log of the number of diagnostic tests carried out systematically to regulate the spread of a particular disease.	Beverelli and Ticku (2025)
Surveillance	Log of the number of measures to continuously investigate a given population to detect the occurrence of disease for control purposes.	– ''–
Human infections	Number of humans infected by animal diseases in grid cell c in year t.	FAO EMPRES-i
REDD+	Equals 1 if the country is a developing country located in a subtropical or tropical area that has signed a Participation Agreement to participate in the Readiness Fund (REDD+).	UNFCC

Notes: Variables are in order of where they appear in Tables 1 and 3 and in Figure 7 in the main text. FAO (Food and Agriculture Organization) EMPRES-i data are available at https://empres-i.apps.fao.org/general. Berman et al. (2023) data are available at https://zenodo.org/record/7044013. Du et al. (2025) data are available at https://zenodo.org/records/11545701. The Uppsala Conflict Data Program Georeferenced Event Dataset (UCDP GED) Global version 25.1 is available at https://ucdp.uu.se/downloads. Liu et al. (2024) data are available at https://zenodo.org/records/11179644. Li et al. (2020) data are available at https://doi.org/10.6084/m9.figshare.9828827.v8. Meijer et al. (2018) data are available at https://www.globio.info/download-grip-dataset. Beverelli and Ticku (2025) data are available at https://doi.org/10.1016/j.worlddev.2025.106969. REDD+ countries are listed at https://redd.unfccc.int/.

Table A.2: Estimation-sample descriptive statistics

Variable	Mean	Median	Std Dev	Min	Max	Number of		
						< 0	Zeros	> 0
Sample: Column 3 of Table 1								
Infection cases	834.02	0	39,207.34	0	3,648,404	0	14,357	1,888
Neighbouring cells deforestation*	9.93	10.60	2.51	-4.61	14.26	50	0	16,195
Own deforestation*	6.85	7.92	3.77	-4.61	13.37	868	0	15,377
Sample: Column 5 of Table 1; Table A.4								
Livestock headcount*	14.61	15.37	2.76	-4.61	19.95	46	0	16,199
Conflict fatalities	1.78	0	27.92	0	2,027	0	15,213	1,032
Temperature	24.18	25.13	3.60	8.03	29.88	0	0	16,245
Rainfall	1,684.14	1,558.60	835.33	278.10	6,888.80	0	0	16,245
Population*	12.20	12.36	1.66	0.01	16.90	0	0	16,245
Nightlights	3.87	1.62	5.97	0	57.51	0	1,855	14,390
Screenings*	0.91	2.08	3.15	-4.61	5.36	3,693	0	12,552
Surveillance*	1.07	2.30	3.12	-4.61	5.28	3,414	0	12,831
Sample: Column 7 of Table 1; Column 1 of Table 3; Table A.3								
Neighbouring cells price index*	4.18	4.18	0.28	3.42	4.97	0	0	16,245
Neighbouring cells price index (5 least suitable crops)*	3.37	4.63	3.10	-4.61	5.50	2,070	0.00	14,175
Infection cases in eight diseases	1,286.94	0	49,078.21	0	3,648,404	0	9,061	1,304
Sample: Column 4 of Table 3								
Infection cases (excl. wildlife)	804.16	0	40,175.07	0	3,648,404	0	9,826	1,184
Neighbouring cells wildlife cases dummy	0.01	0	0.09	0	1	0	10,922	88
Neighbouring cells road density dummy	0.50	1	0.50	0	1	0	5,490	5,520
Sample: Column 1 of Table A.4								
Neighbouring cells deforestation (25)*	10.44	10.73	1.88	-4.61	14.28	15	0	12,615
Own deforestation (25)*	7.74	8.22	2.69	-4.61	13.37	185	0	12,445
Sample: Column 2 of Table A.4								
Neighbouring cells deforestation (IHS)	59.53	65.41	22.49	0	102.37	0	42	12,588
Own deforestation (IHS)	7.62	8.44	3.21	0	14.06	0	693	11,937
Sample: Column 4 of Table A.4								
Infection cases (no zero replacement)	7,907.68	3	128,244.10	0	3,648,404	0	550	953
Sample: Figure 7								
Human infections	3.18	0	48.08	0	1,503	0	1,673	230
Sample: Figure 8								
REDD+	0.94	1	0.23	0	1	0	900	15,345

Notes: Variables marked with * are in logs. See Section 2 and Table A.1 for variables' description.

A.2 Placebo IV: Price index of least suitable crops

We use the relative suitability measure to identify the 5 least suitable crops, among fifteen, for each neighbouring cell of cell c. For these crops we compute the price index for a neighbouring

Table A.3: Placebo IV

	First Stage (1)	Reduced Form (2)
Neighbouring price index (5 least suitable crops)	-0.00706	-5.118
	(0.0252)	(3.829)
Cell FE	Yes	Yes
Year FE	Yes	Yes
Estimator	OLS	PPML
Number of cells	1,083	1,083
Number of countries	60	60
Observations	16,245	16,245

Notes: *p<0.10, **p<0.05,***p<0.01. Dependent variable: Total deforestation in the neighbourhood of cell c in year t (column 1) and Number of animal infection cases in cell c in year t (column 2). Price index is computed as the average price index of least 5 suitable crops for each neighbouring cell c in year t. Years: 2004-2018. See Section 2 and Table A.1 for variables' description.

cell in a year and thus compute the average crop price index of 5 least suitable crops across cells in the neighbourhood of cell c in year t. Table A.3 shows that the placebo IV is neither correlated with neighbourhood deforestation, nor does it affect animal infections in cell c in a year. Given international crop prices do not move the outcome variable and the endogenous variable, when they are not anticipated to raise agricultural demand, bolsters the internal validity of our instrument.

A.3 Distance-based neighbourhood exposure (finer rings)

Figure A.9 shows the impact of neighbouring deforestation in 50 km concentric circles, up to 500 km, and excluding own cell deforestation. Results suggest a local effect: deforestation in 50 km neighbourhood positively affects infections while the rest of the bins are statistically not different from zero.

Figure A.9: Distance-based deforestation exposure

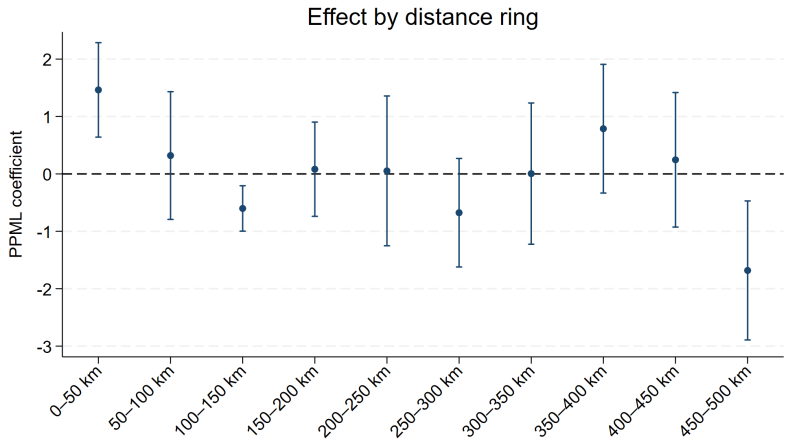

Notes: Dependent variable: Number of animal infection cases in cell c in year t. Years: 2004–2018. Standard errors clustered by cell in parentheses. 95% confidence intervals are reported by the vertical bars.

A.4 Robustness checks

In Tables A.4 and A.5, we assess whether the baseline results are sensitive to alternative definitions of deforestation, sample composition, the treatment of zeros, the inclusion of surveillance controls, and alternative approaches to inference. Since all specifications include cell-level controls, as well as cell and year fixed effects, the results in Tables A.4 and A.5 should be compared to column 5 of Table 1.

Column (1) of Table A.4 shows robustness to defining forests using a 25% canopy threshold (rather than the baseline 50%). Column (2) reports robust results using the inverse hyperbolic sine transformation of neighbouring deforestation, rather than the log specification. In Column (3), we exclude 2004—the first year of the sample—because it is dominated by the December 2003 outbreak of "mad cow disease" In that year alone, total infections reached 7.8 million, compared to 5.7 million over 2005–2018 combined. Excluding 2004 leaves results largely unchanged.

Column (4) excludes the top 0.5% of positive infection cases to test whether results are driven by a handful of extreme epidemics. The elasticity falls from 1.6 to 0.52, but the coefficient remains significant at the 5% level. This indicates that while major outbreaks amplify the baseline magnitude, the core relationship between neighbouring deforestation and animal infections is not due to outliers.

Column (5) examines sensitivity to the large number of zeros in the dependent variable. In the sample of column 3 of Table 1, out of 16,245 observations, 14,357 are zeros and only 1,888 are positive.[i] Dropping all zero replacements reduces the sample size considerably, but the estimated effect remains very similar to the baseline.

Columns (6)-(7) vary the clustering of standard errors, assuming correlation within provinces and within countries respectively.[ii] Finally, column 8 implements two-way clustering (by cell and year) to address serial correlation; results are unchanged.

[i] Similarly, in the sample of column 5 of Table 1, out of 12,630 observations, the dependent variable has 11,220 zeros and 1,410 positive integers.

[ii] There are 385 provinces in column 7, obtained by spatially matching cells to administrative units in ArcGIS.

Table A.4: Deforestation and diseases: Robustness checks

	Alternative deforestation definitions		Excluding 2004	Excluding outlier events	No zero replacement	Alternative clustering of standard errors		
	(1)	(2)	(3)	(4)	(5)	(6)	(7)	(8)
Neighbouring cells deforestation (25)	1.73***							
	(0.39)							
Neighbouring cells deforestation (IHS)		0.24***						
		(0.06)						
Neighbouring cells deforestation			1.45***	0.52**	1.72***	1.72***	1.72***	1.72***
			(0.35)	(0.21)	(0.25)	(0.50)	(0.36)	(0.39)
Cell FE	Yes	Yes	Yes	Yes	Yes	Yes	Yes	Yes
Year FE	Yes	Yes	Yes	Yes	Yes	Yes	Yes	Yes
Own cell controls	Yes	Yes	Yes	Yes	Yes	Yes	Yes	Yes
Clustering of s.e.	Cell	Cell	Cell	Cell	Cell	Province	Country	Cell & Year
No. of cells	1,083	1,083	1,058	1,083	505	1,083	1,083	1,083
No. of countries	60	60	60	60	43	60	60	60
Observations	16,245	16,245	14,812	16,235	2,085	16,245	16,245	16,245

Notes: *p<0.10, **p<0.05,***p<0.01. PPML regressions. Dependent variable: number of animal infection cases in cell c in year t. All regressions include own-cell controls: own deforestation (matching the neighbouring deforestation definition used), livestock headcount, conflict fatalities, temperature, rainfall, trade shock, and nightlights. Column 1 defines forests using a 25% canopy threshold; column 2 uses the inverse hyperbolic sine transformation of neighbouring deforestation; column 3 excludes 2004; column 4 excludes outlier outbreaks (top 1% of positive infection cases); column 5 uses no zero replacement in infections; columns 7-9 vary clustering of standard errors. Years: 2004–2018. See Section 2 and Table A.1 for variables' description.

Table A.5 explores spatial dependence more directly by clustering standard errors on distance-based blocks. Specifically, we partition the study area into blocks of 50, 100, 250, and 500 km (using great-circle scaling, 1 degree = 111.3 km), assign each cell to a block, and cluster at that level. We use block clustering because Conley (HAC) standard errors are not available for PPML in Stata. The results and confidence intervals remain stable across all cutoffs; even at 500 km there are 146 clusters, comfortably above small-sample thresholds, so wild-cluster bootstrapping is not required.

Table A.5: Deforestation and diseases: Spatial autocorrelation

Cluster size	50 km	100 km	250 km	500 km
	(1)	(2)	(3)	(4)
Neighbouring cells deforestation	1.652***	1.652***	1.652***	1.652***
	(0.347)	(0.353)	(0.400)	(0.413)
Cell FE	Yes	Yes	Yes	Yes
Year FE	Yes	Yes	Yes	Yes
Own-cell controls	Yes	Yes	Yes	Yes
Clusters	1,083	712	313	146
Observations	16,245	16,245	16,245	16,245

Notes: *p<0.10, **p<0.05,***p<0.01. PPML regressions. Dependent variable: number of animal infection cases in cell c in year t. Own-cell controls: livestock headcount, conflict fatalities, temperature, rainfall, population, and nightlights. Years: 2004–2018. See Section 2 and Table A.1 for variables' description. We allow for spatially correlated errors by clustering on distance-based blocks (50–500 km).

A.5 Alternative definition of neighbourhood deforestation shocks

In this subsection, we use a narrower threshold to define a deforestation shock in the neighbourhood, such that the biggest year-on-year neighbourhood change is in top 10 percentile of the sample. The dynamics for animal infections and human infections are presented in Figure A.10 and Figure A.11 respectively. The patterns are similar to our baseline event study estimates.

Figure A.10: Neighbourhood deforestation spikes and diseases

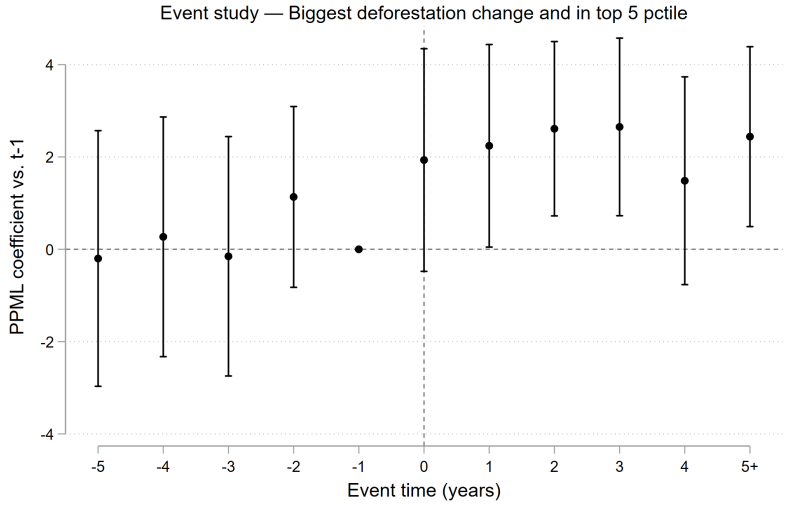

Notes: The figure showcases the dynamics of animal infections around the time of a large deforestation spike in the neighbourhood, as detailed in equation 5. Cell and year fixed effects, along with own-cell controls are included in the estimation. 95% confidence intervals are reported by the vertical bars. Event time -1 is set as the reference period and hence not included in the estimation.

Figure A.11: Neighbourhood deforestation spikes and zoonotic transmissions

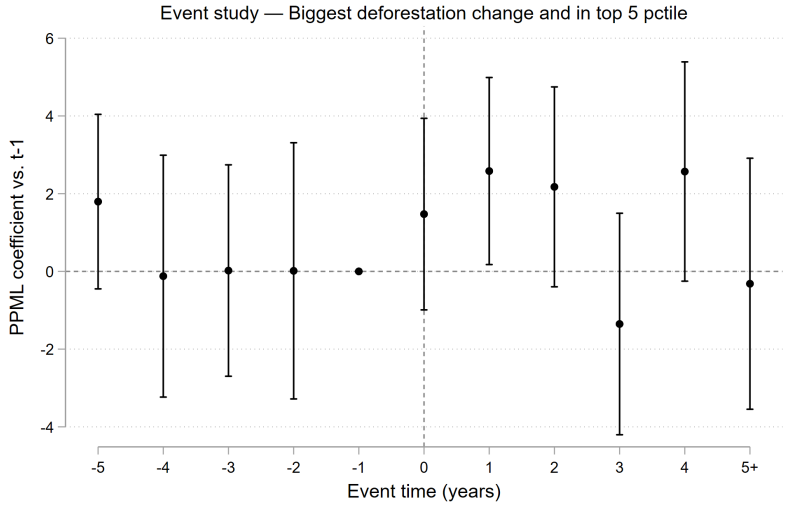

Notes: The figure showcases the dynamics of human infections around the time of a large deforestation spike in the neighbourhood, as detailed in equation 5. Cell and year fixed effects, along with own-cell controls are included in the estimation. 95% confidence intervals are reported by the vertical bars. Event time -1 is set as the reference period and hence not included in the estimation.

A.6 REDD+ countries

Figure A.12 shows the countries in the estimation sample that are part of REDD+ group.

Figure A.12: REDD+ vs non-REDD+ countries

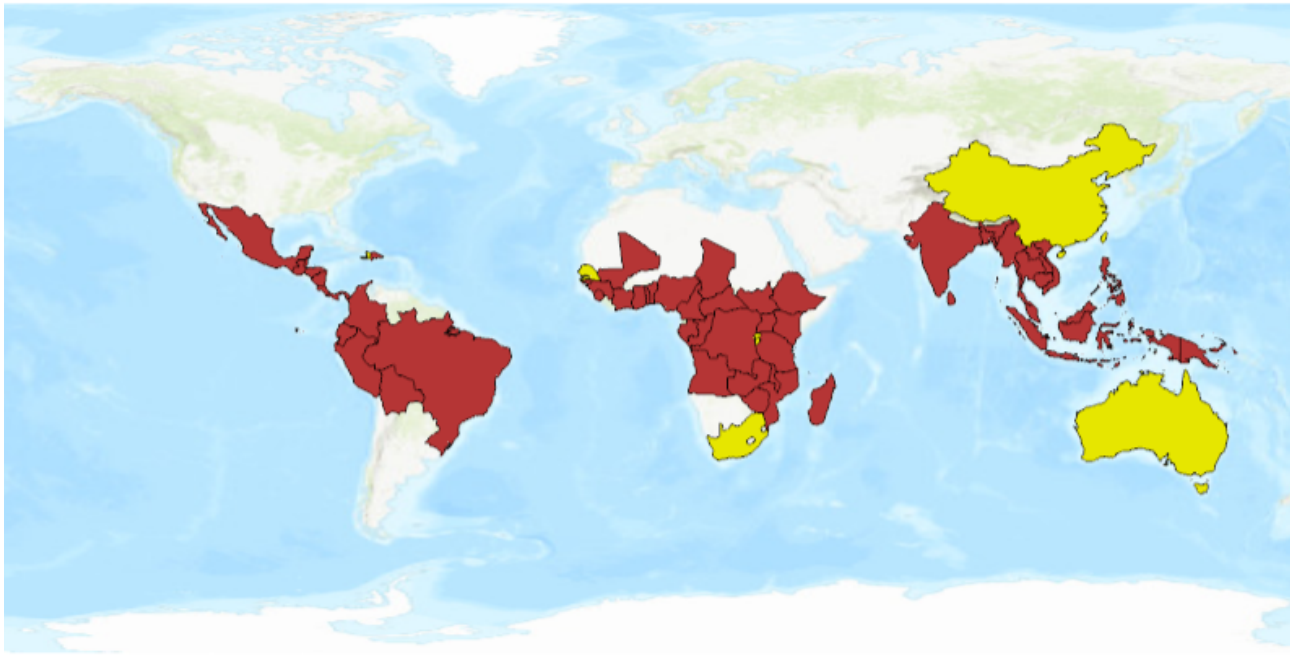

Notes: The coloured part of the world map covers countries that are part of estimation sample in column 5 of Table 1. Redd+ countries are highlighted in red, while non-REDD+ countries are shown in yellow. The data on REDD+ countries is collected from https://redd.unfccc.int/.

Authors

Cosimo Beverelli

University of Modena and Reggio Emilia

cosimo.beverelli@unimore.it

Rohit Ticku

European University Institute

rohit.ticku@eui.eu